Mitotic bypass and endocycling promote cancer cell survival after genotoxic chemotherapy

Kevin Truskowski[1, 2], Louis Rolle[1], George Butler[1, 3], Margaret E Yang[1], Kenneth J Pienta[1, 2], Sarah R Amend[1, 2]

Corresponding Authors: Kevin Truskowski**,** Sarah R Amend

Affiliations:

1. Cancer Ecology Center, The Brady Urological Institute, Johns Hopkins School of Medicine, Baltimore, MD 21287, USA.
2. Cellular and Molecular Medicine Graduate Program, Johns Hopkins School of Medicine, Baltimore, MD 21287, USA.
3. University College London, Cancer Institute, London WC1E 6DD, UK.

Abstract

Genotoxic chemotherapies are central components of the treatment regimen for most cancers but are rarely curative. Drug-tolerant persister cells (DTPs) evade cell death during these treatments by accessing transient adaptive states, allowing them to contribute to cancer progression after treatment. Here, we demonstrate that cancer cells can survive genotoxic chemotherapy-induced stress by accessing a previously undescribed DTP state where mitotic bypass and continued endocycling promote survival by allowing cells to evade mitotic catastrophe and cell death. Mechanistic studies indicate that mitotic bypass is dependent on CDK1 inhibition by WEE1 and Myt1, which prevents entry into mitosis and induces premature APC/C activation during G2 arrest. Disrupting WEE1 or Myt1 activity using clinical-stage small molecule inhibitors promotes CDK1 reactivation, forcing mitotic entry, catastrophe, and cell death. Our results identify mitotic bypass and endocycling as a targetable mediator of cancer cell persistence that can be exploited for the eradication of DTPs.

Introduction

Genotoxic chemotherapies are central tools for the treatment of most cancers. These drug regimens commonly induce initial tumor regression but are rarely curative, leaving behind populations of cancer cells that survive, multiply, and lead to relapse. Understanding which cancer cells survive treatment and how they do so remains an urgent question for the field. Resistance to chemotherapy has largely been attributed to models of genetic heterogeneity whereby a subpopulation of cells harboring a preexisting genetic alteration is selected for under therapeutic pressure, expands, and becomes the dominant population in the persistent tumor. While evidence supporting this model is plentiful, it has become clear that non-genetic mechanisms of resistance are also common[1].

In lieu of genetic advantage, drug-tolerant persister cells (DTPs) survive drug treatment by accessing transient adaptive states, can go on to seed recurrence, and are increasingly recognized drivers of cancer lethality[2,3]. DTPs have been described in various cancer models, including lung, pancreatic, prostate, breast, and melanoma, and in response to both targeted therapies (e.g., kinase inhibitors) and cytotoxic drugs (e.g., platinum-based chemotherapy)[3]. The plastic nature of cancer cells and their ability to quickly adapt to diverse stressors highlights the importance of these states in determining treatment outcome. Insights into the origins and mechanistic control of these adaptive states are critical for expanding our understanding of cancer progression, cancer cells' response to current treatments, and to inform future treatment options for patients.

Here, we demonstrate that genotoxic chemotherapy induces mitotic bypass and endocycling in cancer cells. Prolonged CDK1 inhibition in these cells is sufficient to induce anaphase-promoting complex/cyclosome (APC/C) reactivation during G2 and progression directly into G1 with 4N DNA content (4N-G1). Critically, the cells that survive long-term after drug treatment do not exit the cell cycle but instead enter an endocycle and continue to progress through G1, S, and G2 phases without entering mitosis. The continued bypass of mitosis during the chemo-induced endocycle imparts a fitness advantage, allowing cells to circumvent mitotic catastrophe and cell death in the presence of persistent DNA damage. We show that WEE1- and Myt1-dependent CDK1 inhibition are the critical regulators of stress-induced mitotic bypass, revealing a unique targetable vulnerability. Inhibition of either WEE1 or Myt1 using clinical-stage small molecule inhibitors forces widespread mitotic entry, catastrophe, and cell death. Our findings provide new insight into cancer cell cycle control, introduce the drug-tolerant endocycling persister (DTeP) phenotype as a novel mediator of chemotherapy resistance, and identify WEE1 and Myt1 as clear therapeutic targets for DTeP eradication.

Results

Genotoxic chemotherapy induces widespread mitotic bypass and endoreplication

To monitor cell cycle dynamics in cancer cells responding to genotoxic stress, we engineered cancer cell lines PC3 (prostate), DU145 (prostate), and MDA-MB-231 (breast) to express the Ki67-T2A-FUCCI reporter[4]. The reporter consists of a mCherry-Cdt1 degron and a mAG-Geminin degron, which mark G1 and S/G2/M phases, respectively. Expression of the reporter is driven by the Ki67 promotor, and quiescent G0 cells (Ki67$^-$) are therefore mCherry$^-$/mAG$^-$. The levels of each fluorescent reporter are controlled by anaphase promoting complex/cyclosome (APC/C) activity, which directly degrades mAG-Geminin and indirectly leads to accumulation of mCherry-Cdt1. Therefore, while APC/C activity is high during G1, cells are mCherry^{high}/mAG^{low} and while APC/C activity is low during S, G2, and M, cells are mCherry^{low}/mAG^{high} (**Fig. 1A, B**). Timelapse imaging of PC3-FUCCI, DU145-FUCCI, and MDA-MB-231-FUCCI revealed that instead of cell death, G2 arrest, or progression into mitosis, many cells prematurely reactivate APC/C during stress-induced G2 arrest and progress directly into G1 from G2 without entering mitosis. Mitotic bypass was frequent in all three cell lines in response to the commonly used chemotherapeutics cisplatin, etoposide, and doxorubicin (**Figs. 1C; S1A, B**).

To quantify the frequency of mitotic bypass occurring in response to genotoxic stress, cells were treated for 72h with cisplatin, etoposide, or doxorubicin; drug was washed out and cells that survived 24h later were fixed, immunostained with antibodies against endogenous geminin, and counterstained with diamidino-2-phenylindole (DAPI) to measure DNA content (**Fig. 1D**). Fluorescence intensities were extracted from individually segmented nuclei to enable detailed analysis of the cell cycle state of each cell: 2N, geminin$^-$ cells are in G1; between 2N and 4N, geminin$^+$ cells are in S; 4N, geminin$^+$ cells are in G2; 4N, geminin$^-$ cells have bypassed M into 4N-G1; and cells with >4N DNA content have undergone a subsequent S phase and endoreplication after M bypass (**Fig. 1E**). Strikingly, the majority of PC3 that survive after cisplatin, etoposide, or doxorubicin treatments had bypassed mitosis (**Fig. 1F, G**). Similarly, the majority of MDA-MB-231 and DU145 that survived etoposide or doxorubicin treatment had bypassed mitosis, though cisplatin induced lower levels of bypass in these cells (**Fig. S1C, D**). In contrast to previous reports that such mitotic bypass induces terminal senescence[5], many of these cells that bypassed mitosis had already entered a subsequent S phase and undergone endoreplication, revealing an alternative fate to therapy-induced senescence (**Figs. 1G; S1C, D**- dark red bars).

Many cells that die in response to these drugs do so after failing to maintain G2 arrest, entering mitosis with damaged DNA, and undergoing mitotic catastrophe[6] (**Fig. 1H**). Therefore, M bypass imparts a fitness advantage by allowing chemo-damaged cells to circumvent mitotic cell death. Taken together with previous reports showing the emergence of polyploid cells in various other cancer models

after other drug treatments[7-9], the prevalence of M bypass in our data demonstrates that commonly used genotoxic chemotherapies induce widespread mitotic bypass and endoreplication, suggesting it is a broadly utilized tolerance mechanism in cancer cells (**Fig. 1I**).

Cells that persist after genotoxic chemotherapy enter an endocycle

To determine the cell cycle dynamics and fates of surviving cells that persist after genotoxic damage, we continued to image PC3-FUCCI after 72h cisplatin treatment and drug washout. Surprisingly, virtually all surviving cells remain Ki67$^+$ and therefore continue to express the Ki67-FUCCI reporter, demonstrating that G0 cell cycle exit and/or terminal senescence are uncommon in these persistent cells. We tracked reporter expression in 196 surviving PC3-FUCCI for the 72 hours following cisplatin washout and found that 164/196 (>83%) of these cells bypassed mitosis (mAG-Geminin degradation without mitotic entry) over this timeframe (**Fig. 2A**), demonstrating that most cells continue to bypass mitosis even after the stressor is removed.

The drug doses used in these experiments result in 50% relative viability in treated groups compared to untreated controls after 72h treatment (LD_{50}), as described in the methods. In the days following drug removal, cells continue to die such that by 5 days post-drug washout, the surviving fraction is <10% of that at the end of treatment, as described previously[10]. Strikingly, at this point 5 days post-treatment with cisplatin, etoposide, or doxorubicin, an average of 99.7%, 99.7%, and 99.8% of surviving PC3 had bypassed mitosis, respectively, based on analysis of DNA content and geminin abundance (**Fig. 2B, C**). Similarly, by the same analysis, 92.9%, 85.2%, and 74.1% of MDA-MB-231 had bypassed mitosis 5 days-post treatment with cisplatin, etoposide, or doxorubicin, respectively (**Fig. S2A, B**). These data demonstrate that while cells continue to die after treatment, the surviving fraction is overwhelmingly comprised of cells that have successfully bypassed mitosis.

We continued to observe proliferative arrest but active cell cycle progression in surviving cells for weeks after drug removal, as demonstrated by continued FUCCI reporter oscillation during time-lapse imaging of PC3-FUCCI (**Fig. 2D**). To confirm that FUCCI reporter oscillation accurately reported cell cycle transitions through G1-S-G2, surviving cells were pulsed with 5-ethynyl-2'-deoxyuridine (EdU) 1, 5, and 12 days after 72h cisplatin treatment and washout. At each timepoint, cells actively incorporated EdU (**Fig. S2C**). Further, DNA content continued to increase after drug washout, demonstrating that these non-proliferative cells were continuing to undergo active DNA replication during endocycle S phase (endo-S), as the FUCCI imaging suggested (**Fig. S2D**).

Together, these data demonstrate that after surviving treatment by bypassing mitosis, persistent cells enter an endocycle, where G1, S, and G2 phases proceed in the absence of mitosis (**Fig. 2E**). In

addition to the avoidance of mitotic catastrophe, it is known that actively endocycling cells are resistant to DNA damage-induced apoptosis[11] and that resulting polyploidy confers a survival advantage under conditions of DNA damage[12-15]. The dominance of non-proliferative but actively endocycling cells after these treatments demonstrates that the chemo-induced endocycle is an adaptive phenotype that is strongly selected for in the presence of chemotherapy-induced genotoxic stress. We propose that these drug-tolerant endocycling persisters (DTePs) represent a common but previously unrecognized DTP population.

p21 is dispensable for chemo-induced G2 arrest and mitotic bypass

Bypass of mitosis involves 1) inhibition of G2-M progression and 2) premature APC/C reactivation during G2. Since G2-M progression is controlled by CDK1 activity, we first sought to determine the mechanism of CDK1 inhibition in these cells. Previous reports have demonstrated that p53 and its effector p21 can induce mitotic bypass in response to various cellular stresses by inhibiting CDK1[16-18]. Despite lacking wild-type p53 (PC3: A138fs/del; DU145: P223L/V274F; MDA-MB-231: R280K/R280K), the cell lines in which we observe this response increase p21 expression at both the mRNA and protein level in response to both cisplatin and etoposide by an unknown mechanism (**Fig. S3A-D**). Upregulation of p21 protein appears to be cell cycle phase-independent, with strong upregulation observed in surviving PC3 in all cell cycle phases after 72h etoposide treatment (**Fig. S3E**).

Because of its previously reported role in mitotic bypass, we asked whether p53-independent p21 expression was controlling the endocycle phenotype in our models. If this were the case, then overexpression of p21 alone should be sufficient to induce mitotic bypass and endocycling. To test this, we introduced a Tet-inducible *CDKN1A* overexpression construct into PC3 (hereafter termed PC3-p21OE). PC3 and PC3-p21OE were treated +/- doxycycline for 72hr, which induced a strong upregulation of p21 protein in PC3-p21OE (**Fig. S3F**). Cells were fixed, immunostained for geminin, and counterstained with DAPI as in (**Fig. 1C**) to quantify the fraction of cells that had bypassed mitosis. Induction of p21 expression did not induce significant change in the fraction of cells bypassing mitosis (**Fig. S3G**), suggesting that p21 upregulation alone is not sufficient to explain the observed chemo-induced M bypass.

To determine whether p21 upregulation is required for stress-induced mitotic bypass, we introduced shRNA targeting *CDKN1A* to knock down p21 expression during drug treatment. PC3-scrRNA and PC3-sh*CDKN1A* were treated for 72hr with DMSO or etoposide +/- doxycycline to induce shRNA expression. Etoposide treatment induced the expected upregulation of p21 protein and mitotic bypass. Concurrent doxycycline treatment reduced p21 protein levels to that of DMSO-treated controls

but did not impair etoposide-induced mitotic bypass (**Fig. S3H, I**). Together, these data demonstrate that chemo-induced mitotic bypass is p21-independent and led us to examine other mechanisms of CDK1 inhibition.

WEE1-, Myt1- dependent CDK1 inhibition is required for G2 arrest and mitotic bypass

In the absence of functional p53, cells rely on alternate mechanisms to control CDK activity and halt cell cycle progression into mitosis when DNA damage is sensed. In addition to interaction with cyclin-dependent kinase inhibitors (CDKis) like p21, CDK1 can be inhibited by phosphorylation at Thr14 or Tyr15 by Myt1 and WEE1, respectively[19,20]. In response to both cisplatin and etoposide, we observed an increase in phosphorylation of both phospho-marks on CDK1 in PC3, MDA-MB-231, and DU145 suggesting a role for them in mitotic bypass (**Figs. 3A; S4A, B**).

To confirm that CDK1 phosphorylation is carried out by WEE1 and Myt1, we treated PC3 with cisplatin or etoposide for 24h to induce stress, CDK1 phosphorylation, and G2 arrest (**Fig. 3B**) then added WEE1 or Myt1 inhibitors (WEE1i, Myt1i) for an additional 24h and assessed CDK1 phosphorylation by Western Blot (**Fig 3C**). As expected, Myt1i and WEE1i reduced CDK1 phosphorylation at T14 and Y15, respectively. Inhibiting ataxia telangiectasia and Rad3 related (ATR), the upstream activator of WEE1, had a similar effect to WEE1i, though was more modest. Inhibiting ataxia telangiectasia mutated (ATM), a central coordinator of the response to DNA double-strand breaks, had no effect on CDK1 phosphorylation (**Fig. 3D**). Together, this demonstrates that CDK1 phosphorylation is specifically controlled by Myt1 and ATR-WEE1 signaling, and that we can disrupt stress-induced CDK1 phosphorylation using inhibitors against Myt1, ATR, and WEE1.

We hypothesized that CDK1 inhibition drives mitotic bypass, an adaptive survival mechanism in response to genotoxic stress. If WEE1- or Myt1-dependent CDK1 phosphorylation were critical for G2 arrest and subsequent mitotic bypass, then their inhibition during stress-induced G2 arrest should lead to CDK1 reactivation, forcing mitotic entry, catastrophe, and cell death. To test the functional consequences of impairing CDK1 phosphorylation, PC3-FUCCI were treated as in (**Fig. 3C**) and time-lapse imaged following the addition of inhibitors. The resulting time series images were used to annotate cell fates. Analysis was limited to those cells that were G2-arrested at the start of inhibitor treatment to specifically investigate the effects of inhibitors on stress-induced G2 arrest. Six distinct cell fates were observed in these experiments: successful mitoses, continued G2 arrest, cell death outside of mitosis, endo-mitosis (mitotic entry then exit before karyokinesis, resulting in a 4N-G1 cell with an intact nucleus), mitotic bypass (mAG-geminin degradation without mitotic entry), and mitotic catastrophe (either cell death during mitosis or mitotic entry followed by failed karyokinesis, resulting in

a single G1-like cell with highly fragmented nuclei, which die within hours of mitotic failure) (**Fig. S4C**). In these experiments, inhibition of Myt1, WEE1, ATR, or ATM had little effect on the fates of unstressed, DMSO-treated controls, where most cells completed successful mitoses (**Fig. 3E**). In G2 cells harboring damage from cisplatin or etoposide treatment, the addition of WEE1, Myt1, or ATR inhibitors, which disrupt CDK1 phosphorylation (**Fig. 3D**), induced widespread G2 checkpoint failure and mitotic catastrophe (**Fig. 3F, G**; left). ATM inhibition, which does not impair cisplatin- or etoposide-induced CDK1 phosphorylation (**Fig. 3D**), did not impact G2 arrest, mitotic bypass, or survival in these cells (**Fig. 3F, G**; left), demonstrating a specific reliance on CDK1 phosphorylation by Myt1 or ATR-WEE1. Importantly, the addition of a CDK1 inhibitor (CDK1i) in combination with WEE1i, Myt1i, and ATRi completely reversed their effects demonstrating that the results are dependent on CDK1 activity (**Fig. 3F, G**; right).

Together, these data demonstrate that WEE1- and Myt1-dependent CDK1 phosphorylation controls G2 arrest and mitotic bypass in these p53-deficient cancer cells in response to genotoxic stress (**Fig. 3H**). Critically, the dependence of these cells on WEE1 and Myt1 activity uncovers a vulnerability that can be exploited to prevent M bypass and instead force extensive mitotic catastrophe, dramatically reducing the fraction of surviving cells after chemotherapy treatments.

CDK1 inhibition is sufficient to induce G2 arrest and premature APC/C reactivation

In addition to CDK1 inhibition, mitotic bypass involves premature APC/C reactivation during G2 arrest. In previous experiments, we observed that CDK1i treatment not only rescued the effects of inhibitors in cisplatin- or etoposide-stressed cells, as described, but also induced widespread M bypass in unstressed, DMSO-treated cells (**Fig. 3E**), suggesting that CDK1 inhibition alone is sufficient to induce premature APC/C activation. To confirm this, PC3-FUCCI, DU145-FUCCI, and MDA-MB-231-FUCCI were treated with CDK1 inhibitor Ro-3306[21] and timelapse imaged for 72h. In all three cell lines, CDK1i induced extensive APC/C reactivation during G2, leading to mAG-Geminin degradation and mitotic bypass. Most of these cells then proceeded to re-enter S-phase (**Fig. 4A; S5A**). Geminin immunostaining of PC3 after 72h CDK1i treatment further confirmed that CDK1i alone induces widespread M bypass (>75% of cells) and endoreplication (58.2% of cells), with cells reaching ploidies up to 32N (**Fig. 4B, C**). Similar levels of M bypass occurred in MDA-MB-231 and DU145 after 72h CDK1i treatment (**Fig. S5B, C**). We next asked whether this was a universal response to inhibition of CDK activity. In contrast to CDK1i, neither CDK4/6 nor CDK2 inhibition (CDK4/6i, CDK2i) induced appreciable mitotic bypass or endoreplication in PC3 (**Fig. 4B, C**), demonstrating that prolonged CDK1

inhibition, but not CDK4/6 or CDK2 inhibition is sufficient to induce premature APC/C reactivation on its own.

Multiple recent studies have demonstrated that CDK2 and CDK4/6 activities are critical for preventing premature APC/C reactivation during G2[22-24]. Thus, we sought to test the roles of CDK2 and CDK4/6 activities in chemo-induced M bypass. If CDK2 and/or CDK4/6 act to prevent APC/C reactivation during G2 arrest in chemo-treated cells, then inhibiting them during chemo-induced G2 arrest should promote M bypass, as was shown previously in the context of other stress conditions[23]. To test this, G2 arrest was induced by treating cells for 24h with cisplatin, etoposide, or CDK1i (**Fig. 3B, S5D, E**) before adding CDK2i or CDK4/6i for 24h. Geminin and DNA content were analyzed to quantify the levels of M bypass in each condition (**Fig 4D**).

In PC3, CDK2i alone induced low levels of bypass in unstressed, DMSO-treated controls, and did not increase M bypass in response to cisplatin, etoposide, or CDK1i (DMSO vs. CDK2i: 25.8% vs. 9.4%; 33.3% vs. 32.6%; and 72.1% vs. 75.1% in cisplatin, etoposide, and CDK1i-treated cells, respectively) (**Fig. 4E**). Similar results were obtained in MDA-MB-231 (**Fig S5F**). CDK2, like CDK1, is a WEE1 target, and we reasoned that stress from cisplatin and etoposide treatments could lead to CDK2 inhibition, rendering CDK2i treatment redundant. Indeed, WEE1-dependent CDK2 phosphorylation (inhibition) is induced in both cisplatin- and etoposide- treated PC3 (**Fig. S5G**). Since CDK2 is already inhibited by cisplatin- and etoposide-induced genotoxic stress, adding a CDK2 inhibitor may be redundant and explain its lack of effect in this assay.

Inhibiting CDK4/6 during cisplatin-, etoposide-, or CDK1i- induced G2 arrest (**Fig 4D**) only modestly increased the percent of cells that underwent M bypass (DMSO vs. CDK4/6i: 25.8% vs. 32.9%; 33.3% vs. 44.8%; and 72.1% vs. 77.9% in cisplatin, etoposide, and CDK1i-treated cells, respectively). Similar effects were seen in MDA-MB-231 (**Fig. S5F**). We asked whether, like CDK2, CDK4/6 activity is also being inhibited by cisplatin or etoposide stress alone, making CDK4/6i redundant in these experiments. By evaluating phosphorylation levels of CDK4/6 target Rb, we find that, as expected, cells in G1 phases have low CDK4/6 activity but CDK4/6 is still activated in late G1, S and G2 phases under cisplatin and etoposide treatment. The phosphorylation pattern in cisplatin- or etoposide- treated cells resembles that in CDK1i-treated cells, which induces M bypass but should not influence CDK4/6 activity (**Fig. S5H**). Therefore, unlike in CDK2i conditions, the modest effect of CDK4/6 inhibition during G2 arrest in these experiments cannot be explained by redundant CDK4/6 inhibition.

Taken together, these results demonstrate that CDK1 inhibition alone is sufficient to induce widespread M bypass. The modest effect of CDK4/6i on levels of M bypass in stressed cells combined

with the widespread M bypass induced by CDK1i treatment alone suggests that chemo-induced CDK1 inhibition is the major driver of G2 arrest and premature APC/C activation in these stress conditions.

Polyploidy and persistent DNA damage induce stress signaling during endo-S phases

The observation that surviving cells continue to endocycle long after drug removal led us to investigate the mechanisms that continue to induce mitotic bypass independent of the acute effects of genotoxic drugs. It is known that polyploidy can induce replication stress during S phase[25]. We therefore hypothesized that stress induced by polyploid endocycle-S (endo-S) phases activates ATR signaling and downstream WEE1-dependent CDK1 phosphorylation, that continues to induce G2 APC/C reactivation and mitotic bypass and maintains the endocycle. We assessed ATR activation in DTePs 8 days after cisplatin or etoposide treatment by immunostaining and quantifying levels of phosphorylation of ATR target checkpoint kinase 1 (Chk1) in individual nuclei. We classified cells as G1 or Post-G1 based on geminin abundance to evaluate whether stress signaling was related to endo-S phase entry, specifically (**Fig. S6A**). Cells surviving stress induced by either cisplatin or etoposide treatment have high levels of pChk1, which are further increased after S phase entry (**Fig 5A, B; S6B**). In addition to ATR activation, these cells have high levels of the DNA double-strand break (DSB) marker γH2AX along with related ATM activation (seen by phosphorylation of its target, checkpoint kinase 2 (Chk2)), which responds to DSBs. On average, levels of γH2AX are similar in G1 and post-G1 populations, suggesting that DNA damage is present prior to, and is not induced as a direct consequence of, endo-S phase, in contrast to a previous report[25] (**Fig. 5C-F; S6C, D**). Instead, we reasoned that persistent DNA damage may be responsible for inducing endo-S phase stress signaling, downstream CDK1 inhibition, and perpetuation of M bypass in DTePs.

To dissect the roles of polyploidy vs. DNA damage in the activation of stress signaling during endo-S phase, we analyzed ATR and ATM activation in CDK1i-induced endocycling cells (CDK1i-ECCs), as 72hr CDK1i treatment induces endocycling and polyploidy without inducing the high levels of DNA damage seen after chemo treatments (**Fig. 5G, H**). CDK1i-ECCs have only slightly elevated levels of p-Chk1 and p-Chk2, on average, and levels are only slightly higher in post-G1 compared G1 cells (**Fig. 5H**), demonstrating that polyploidy alone is only sufficient to induce low levels of S phase stress signaling. These modest increases in phosphorylation of Chk1 (1.01-fold increased) and Chk2 (1.63-fold increased) compared to that in cisplatin- (2.12- and 3.58-fold increases in p-Chk1 and p-Chk2, respectively) or etoposide-treated (1.97- and 2.17-fold increases in p-Chk1 and p-Chk2, respectively) endocycling persisters, suggests that persistent DNA damage during endo-S phase likely plays a larger role in driving stress signaling in DTePs.

WEE1, Myt1 activities are required for endocycling and survival in persistent cells

In the acute response to genotoxic stress, we determined that WEE1 and Myt1 were critical for CDK1 inhibition, mitotic bypass, and survival. Thus, we asked whether WEE1i or Myt1i similarly affected CDK1 phosphorylation in endocycling persisters. In PC3 DTePs 1 or 8 days after cisplatin or etoposide treatment, inhibiting WEE1 or Myt1 strongly decreased Y15 or T14 phosphorylation, respectively, suggesting their activities continue to be required for CDK1 inhibition in endocycling persisters (**Fig. 6A; S7A**). If DTePs continue to depend on the activity of these kinases to perpetuate M bypass and the endocycle, then their inhibition should impair M bypass and instead force cells into catastrophic mitoses. To test this, PC3-FUCCI were treated with cisplatin for 3 days to induce endocycling, drug was washed out, and cells that survived 4 days later were treated with WEE1, Myt1, ATR, or ATM inhibitors and time-lapse imaged over 24h (**Fig. 6B**). Six distinct cell fates were annotated, as in (**Fig. S4C**). Both WEE1i and Myt1i were sufficient to induce widespread mitotic entry and catastrophe. ATRi had a similar effect to that of WEE1i, as expected based on its role in activating WEE1. While inhibition of either WEE1, Myt1, or ATR induced widespread mitotic entry, only Myt1i reduced the percent of cells undergoing mitotic bypass suggesting a specific dependence on Myt1 activity for APC/C reactivation and mitotic bypass in DTePs (**Fig. 6C**; left). Critically, the effects of all three inhibitors were abrogated by adding CDK1i, demonstrating that their effects on cell fate are directly related to their role in CDK1 inhibition (**Fig. 6C**; right). Since these cells have high levels of DNA DSBs and related ATM signaling (**Fig. 5C-F**), we also asked whether, in contrast to its role during the acute response to genotoxic stressors, ATM was involved in CDK1 inhibition or M bypass in endocycling persisters. ATM inhibition had no effect on CDK1 phosphorylation (**Fig. S7B**) or on cell fate (**Fig. S7C**).

Together, these data demonstrate that DTePs continue to have a specific dependence on WEE1 and Myt1 activity to inhibit CDK1, maintain the endocycle, and promote their survival after genotoxic insult. This dependency renders them uniquely vulnerable to WEE1 and Myt1 inhibition, which forces widespread CDK1 reactivation and mitotic catastrophe, offering insight toward eradicating persistent cancer cells.

Discussion

Chemotherapy tolerance and long-term persistence are critical drivers of cancer progression and lethality. Our results show that mitotic bypass resulting from premature APC/C reactivation during genotoxic stress-induced G2 arrest is common and highly selected for in the presence of widely used chemotherapeutics, allowing cells harboring DNA damage to circumvent mitotic catastrophe and cell death. In contrast to other reports of mitotic bypass as a precursor to terminal senescence[5], here, p53-deficient cancer cells that continue to persist after chemotherapy do so in an endocycle: a state of proliferative arrest but active cell cycle, where DNA replication becomes decoupled from cell division. This active cell cycle distinguishes endocycling persisters from classically senescent cells, and it is intriguing to ask whether reports of reversible therapy-induced senescence[26] may involve endocycling. Endocycles are a conserved stress response mechanism known to occur in yeast, drosophila, plants, and mammalian cell types[27-30], but have not been previously described as an adaptive response to chemotherapy in cancer cells. Drug tolerant endocycling persister cells (DTePs) therefore represent a novel DTP phenotype wherein continued endocycling and polyploidy protects against DNA damage-induced apoptosis[11-15].

Continued endocycling and thus survival is likely facilitated, at least in part, due to these cells' lack of p53-dependent checkpoint mechanisms that would otherwise prevent such dramatic polyploidization[25,31]. Since p53 mutation commonly precedes whole-genome doubling (WGD) during tumorigenesis[8], a similar route to stress-induced mitotic bypass and endoreplication may be involved in early WGD, which is widely understood to be a precursor to the aneuploidy and chromosomal instability that can drive cancer initiation and evolution[32]. Drug-induced polyploidy during the treatment of established cancers may then drive similar bursts of evolution that promote recurrence and progression after chemotherapy[33-35]. Recent studies have described the emergence of reversibly polyploid cells in several cancer types in response to various genotoxic stressors[9], demonstrating roles for these cells in invasion[36], metastasis[37,38], and resistance to treatment[10,39]. Future studies are needed to evaluate whether the endocycling mechanism we describe is involved in these negative outcomes.

Our results show that CDK1 inhibition induced by genotoxic stress or by a small molecule CDK1 inhibitor is sufficient to induce widespread premature APC/C activation and mitotic bypass on its own, which leads to endoreplication. Indeed, CDK1 plays a direct role in controlling APC/C activity by phosphorylating Cdc20-homolog 1 (Cdh1) and preventing its association with APC/C[40]. Thus, when CDK1 is inhibited during chemo- or CDK1i- induced G2 arrest, Cdh1 is free to interact with and activate APC/C, driving M bypass. Our data suggest that caution should be taken in the development of CDK1 inhibition as a therapeutic strategy. Though CDK1 inhibition alone may suppress tumor growth, unintended WGD may result in exacerbation of genome instability and treatment resistance. Further,

our results suggest that the combination of CDK1 inhibition with genotoxic agents, as has been proposed for the treatment of metastatic pancreatic cancer[41], for example, may be counterproductive, with CDK1 inhibition promoting M bypass and resistance to DNA damage-induced cell death.

Importantly, we have found that in both the acute response to drug and in the perpetuation of the endocycle in DTePs after drug removal, mitotic bypass is regulated by WEE1- and Myt1-dependent CDK1 inhibition. Continued CDK1 inhibition likely contributes to survival in these cells, as CDK1 activity is required for some forms of apoptosis[42]. Dependence on WEE1 and Myt1 during both the early and late stages of the drug response offers two windows for intervention to eradicate these cells. WEE1 and Myt1 are investigational drug targets and the inhibitors used in our studies are currently being evaluated in clinical trials for the treatment of various cancers. Our results may help to explain the synergistic effects seen with these drugs in combination with DNA damaging agents in preclinical studies[43,44].

Acknowledgements

We would like to thank Dr. Sergi Regot and Dr. Christina Ferrer for helpful discussions. This work was funded by US Department of Defense CDMRP/PCRP (W81XWH-20-10353 and W81XWH-22-1-0680), the Prostate Cancer Foundation, and the Patrick C. Walsh Prostate Cancer Research Fund to SRA; and NIH/NCI P01CA093900 and the Prostate Cancer Foundation to KJP.

Author contributions

KT, KJP, and SRA designed the study; KT, LR, and MEY performed the experiments; KT, LR, and GB analyzed the data, and KT wrote the manuscript with input from KJP and SRA; KJP and SRA acquired funding.

Declaration of interests

The authors declare no competing interests.

Materials and Methods

Cell culture

PC3 (CRL-1435), MDA-MB-231 (CRM-HTB-26), DU145 (HTB-81), and HEK293T (CRL-3216) were purchased from ATCC and cultured according to ATCC recommendations. Flasks were passaged using TrypLE Express (Gibco #12604013) when cells reached 60-80% confluence.

Stable cell line engineering

For FUCCI lines, 1.5e6 293T were plated in 10cm dishes. The following day, cells were transfected for second generation lentivirus packaging as follows: 1ug of Hs.Ki67-T2A-FUCCI plasmid (a gift from Alexander Zambon), 1ug of psPAX2:pMD2.G (both gifts from Didier Trono, Addgene plasmid #12260, 12259) at an 8:1 ratio, and 5uL of X-tremeGENE HP transfection reagent (Roche #6366244001) were combined in 200uL in OptiMEM (Gibco 31985062) and incubated for 30 minutes before adding dropwise to 293T dishes. 18-20hr later, media was changed to target cell media + 30% heat inactivated FBS. Packaging cells were allowed to condition media for 48hr before viral harvest. Viral media was removed and filtered through a Millex HP 0.45um PES syringe filter (Millipore SLHPM33RS). Lentivirus from 1-2 10cm dishes (10-20ml) was concentrated using Clontech Lenti-X concentrator per manufacturer protocol (Takara #631232). 350k target cells were plated per well of a 6-well plate. Following concentration, viral pellet was resuspended in 2ml of target cell media + 30% heat inactivated FBS and moved to target cells in 6 well plate. 10ug/ml Polybrene (Millipore TR-1003) was added directly to well. Target cells were transduced for ~20hr before changing media. After 3 days recovery, cells were selected with 5ug/ml blasticidin (Gibco A1113903) until untransduced control cells were dead.

For inducible p21 overexpression, Gateway donor pDONR223_CDKN1A_WT (a gift from Jesse Boehm & William Hahn & David Root; Addgene plasmid # 82201) was recombined with Gateway destination pLIX_403 (a gift from David Root; Addgene plasmid # 41395) using Gateway LR Clonase II (Invitrogen #11791020) to generate the CDKN1A expression clone.

For inducible p21 knockdown, Tet-pLKO-Neo[45] (a gift from Dmitri Wiederschain; Addgene plasmid # 21916) [CITE] was digested with AgeI (New England Biolabs R3552) and EcoR1 (New England Biolabs R3101), then scrambled or *CDKN1A*-targeting shRNA were inserted using Instant Sticky-end Ligase Master Mix (New England Biolabs M0370) all according to manufacturer's protocol.

Lentivirus packaging and PC3 transduction were carried out as above. 72 hours later, Tet-pLKO-Neo cells were selected with 1mg/ml G418 and pLIX403-CDKN1A cells were selected with 0.5μg/ml puromycin (pLIX403) until untransduced control cells were dead. Expression of shRNAs or CDKN1A

were induced by 1μg/ml doxycycline treatment and knockdown/overexpression were confirmed by Western Blot.

shRNA sequences:

Scr:

CCGGGCGCGATAGCGCTAATAATTTCTCGAGAAATTATTAGCGCTATCGCGCTTTTTG

sh*CDKN1A*:

CCGGCGCTCTACATCTTCTGCCTTACTCGAGTAAGGCAGAAGATGTAGAGCGTTTTTG

Drug treatments

Each cell line was treated for 72 hours with increasing doses of cisplatin (Sigma #232120), etoposide (Cell Signaling Technology #2200), or doxorubicin (Sigma #D1515) and LD50 values were determined by Alamar Blue according to manufacturer's protocol (Invitrogen #DAL1025). The following 72h LD50 values were used for each chemotherapy drug treatment: PC3- 6μM cisplatin, 5μM etoposide, 200nM doxorubicin; MDA-MB-231- 12μM cisplatin, 6μM etoposide, 400nM doxorubicin; DU145- 2μM cisplatin, 1.5μM etoposide, 50nM doxorubicin.

1μM WEE1i (Adavosertib, SelleckChem #S1525), 1μM Myt1i (RP-6306, MedChemExpress #HY145817A), 1μM ATRi (Ceralasertib, #S7693), 1μM ATMi (KU-60019, SelleckChem #S1570), 1μM CDK4/6i (Palbociclib, MedChemExpress #HY50767), 500nM CDK2i (INX-315, SelleckChem #E1854), and 5μM CDK1i (Ro-3306, SelleckChem #S7747) were used unless stated otherwise.

Immunofluorescence Imaging and Cytometry analysis

Cells were cultured in 8- or 12-well chamber slides (Ibidi #80841, 81202). Cells were fixed in 4% paraformaldehyde for 15 minutes, then blocked and permeabilized with 0.3% Triton-X100 + 5% normal goat serum in PBS for 60 minutes. Primary antibody was diluted in PBS containing 1% BSA and 0.3% Triton-X100 and cells were incubated with primary antibody solution overnight at 4°C. After washing 3x 10min in PBS, fluorescent secondary antibodies along with DAPI were diluted in the same antibody buffer, cells were incubated for 60 minutes at room temperature, then washed 3x 10min in PBS before mounting with Prolong Diamond antifade mounting medium (Invitrogen P36970).

Images were acquired using a Zeiss Observer Z1 microscope/ZEN pro 2.0 software (Carl Zeiss Microscopy). Cytometry analysis was performed using CellProfiler and R. Briefly, individual nuclei were segmented based on DAPI signal and intensity values within each nucleus were extracted for each fluorescent channel using CellProfiler. Downstream analysis and data visualization were performed using R.

Primary antibodies against p21 (#2947; 1:200), phospho-Rb S807/11 (#8516; 1:5000), geminin (#52508; 1:1000), phospho-Chk1 S345 (#2348; 1:50), and phospho-Chk2 T68 (#2197; 1:100) were purchased from Cell Signaling Technologies. Anti- geminin (ab104306; 1:25000) and γH2AX (ab22551; 1:10000) were purchased from Abcam. Goat anti-mouse Alexa Fluor Plus 488 (A32723) or Alexa Fluor Plus 555 (A32727), and goat anti-rabbit Alexa Fluor Plus 488 (A32731) or Alexa Fluor Plus 555 (A32732) secondary antibodies were acquired from Invitrogen and used at 1:200.

Immunoblotting

Cells were scraped into ice-cold PBS and pelleted by centrifugation at 5000 x g for 5 minutes. Lysates were collected in RIPA supplemented with protease/phosphatase inhibitors (Cell Signaling Technology #5872). Lysates were clarified by centrifugation at 10000 x g for 15 minutes at 4°C. Protein concentration was measured using Pierce BCA assay (Thermo Scientific #23225) according to manufacturer protocol. Normalized samples were mixed with 4x Laemmli buffer (BioRad #1610747) and boiled at 95°C for 10 minutes before being loaded into 4-20% Bis-tris polyacrylamide gels (BioRad #4561095). Electrophoresis performed with Tris/Glycine/SDS buffer (BioRad #1610732). Protein was transferred to nitrocellulose membranes (BioRad #1704158) using the BioRad TransBlot Turbo system per manufacturer protocol. Membranes were blocked for 60 minutes in StartingBlock buffer (Thermo Scientific #37538). Primary antibody was diluted in Intercept T20 buffer (Licor #927-65001) and membranes were incubated overnight at 4°C with agitation followed by 3x 5min washes with TBST, then incubated 60 minutes in secondary antibody at room temperature, washed 3x 5min with TBST, and imaged with Licor Odyssey imager. Primary antibodies against phospho-CDK1 Y15 (#4539), CDK1 (#9116), p21 (#2947), and CDK2 (#18048) were purchased from Cell Signaling Technology and used at 1:1000. Anti- phospho-CDK T14 (#ab58509) and phospho-CDK2 Y15 (ab314034) were purchased from Abcam and used at 1:1000. Anti- actin (#A5441) was purchased from Sigma and used at 1:5000. Goat anti-Rabbit 800CW (#926-32211) and goat anti-mouse 680RD (#926-68070) secondary antibodies were purchased from Licor and used at 1:20000.

Time lapse imaging

Cells were plated in 96-well ImageLock plates (Sartorius #BA-04856) in phenol-red free medium and imaged every 20 minutes with Incucyte SX5 equipped with Green/Orange/NIR optical module (Sartorius).

qPCR

Cells were rinsed with ice-cold PBS then scraped into 1mL ice-cold PBS and pelleted by centrifugation at 1000 x g for 5 minutes at 4°C. mRNA was isolated using RNeasy Plus kit (Qiagen #74134) and concentration was quantified with NanoDrop One (Thermo Scientific). Reverse transcription of 1ug input mRNA was done using iScript cDNA synthesis kit (BioRad #1708890) according to manufacturer's protocol. Real-time PCR was done using SssoFast EvaGreen (BioRad #1725200) and run on BioRad CFX Opus real-time PCR machine. The following primers were purchased from Integrated DNA technologies: CDKN1A (fwd: CGGAACAAGGAGTCAGACATT; rev: AGTGCCAGGAAAGACAACTAC), ACTB (fwd: CATGTACGTTGCTATCCAGGC; rev: CTCCTTAATGTCACGCACGAT).

EdU incorporation assay

Cells were plated in 8-well chamber slides (Ibidi #80841) and 24h later pulsed with 10uM EdU (Molecular Probes E10187) for 20h. Click-It Plus EdU assay (Molecular Probes C10640) was performed according to manufacturer's protocol then samples were incubated with DAPI for 10 minutes before mounting slides with Prolong Diamond antifade mounting medium (Invitrogen P36970). Images were acquired and analyzed as for Immunofluorescence experiments, above.

Statistical analysis

All statistical analyses were performed in R with $\alpha = 0.05$. Specific comparisons, tests used, and p values are described in each figure legend.

References

1. Marine, J.C., Dawson, S.J., and Dawson, M.A. (2020). Non-genetic mechanisms of therapeutic resistance in cancer. Nat Rev Cancer *20*, 743-756. 10.1038/s41568-020-00302-4.
2. Pu, Y., Li, L., Peng, H., Liu, L., Heymann, D., Robert, C., Vallette, F., and Shen, S. (2023). Drug-tolerant persister cells in cancer: the cutting edges and future directions. Nat Rev Clin Oncol *20*, 799-813. 10.1038/s41571-023-00815-5.
3. Shen, S., Vagner, S., and Robert, C. (2020). Persistent Cancer Cells: The Deadly Survivors. Cell *183*, 860-874. 10.1016/j.cell.2020.10.027.
4. Zambon, A.C., Hsu, T., Kim, S.E., Klinck, M., Stowe, J., Henderson, L.M., Singer, D., Patam, L., Lim, C., McCulloch, A.D., et al. (2020). Methods and sensors for functional genomic studies of cell-cycle transitions in single cells. Physiol Genomics *52*, 468-477. 10.1152/physiolgenomics.00065.2020.
5. Johmura, Y., Shimada, M., Misaki, T., Naiki-Ito, A., Miyoshi, H., Motoyama, N., Ohtani, N., Hara, E., Nakamura, M., Morita, A., et al. (2014). Necessary and sufficient role for a mitosis skip in senescence induction. Mol Cell *55*, 73-84. 10.1016/j.molcel.2014.05.003.
6. Vakifahmetoglu, H., Olsson, M., and Zhivotovsky, B. (2008). Death through a tragedy: mitotic catastrophe. Cell Death Differ *15*, 1153-1162. 10.1038/cdd.2008.47.
7. Trabzonlu, L., Pienta, K.J., Trock, B.J., De Marzo, A.M., and Amend, S.R. (2023). Presence of cells in the polyaneuploid cancer cell (PACC) state predicts the risk of recurrence in prostate cancer. Prostate *83*, 277-285. 10.1002/pros.24459.
8. Bielski, C.M., Zehir, A., Penson, A.V., Donoghue, M.T.A., Chatila, W., Armenia, J., Chang, M.T., Schram, A.M., Jonsson, P., Bandlamudi, C., et al. (2018). Genome doubling shapes the evolution and prognosis of advanced cancers. Nat Genet *50*, 1189-1195. 10.1038/s41588-018-0165-1.
9. Amend, S.R., Torga, G., Lin, K.C., Kostecka, L.G., de Marzo, A., Austin, R.H., and Pienta, K.J. (2019). Polyploid giant cancer cells: Unrecognized actuators of tumorigenesis, metastasis, and resistance. Prostate *79*, 1489-1497. 10.1002/pros.23877.
10. Kim, C.J., Gonye, A.L., Truskowski, K., Lee, C.F., Cho, Y.K., Austin, R.H., Pienta, K.J., and Amend, S.R. (2023). Nuclear morphology predicts cell survival to cisplatin chemotherapy. Neoplasia *42*, 100906. 10.1016/j.neo.2023.100906.
11. Mehrotra, S., Maqbool, S.B., Kolpakas, A., Murnen, K., and Calvi, B.R. (2008). Endocycling cells do not apoptose in response to DNA rereplication genotoxic stress. Genes Dev *22*, 3158-3171. 10.1101/gad.1710208.
12. Hayashi, K., Horisaka, K., Harada, Y., Ogawa, Y., Yamashita, T., Kitano, T., Wakita, M., Fukusumi, T., Inohara, H., Hara, E., and Matsumoto, T. (2024). Polyploidy mitigates the impact of DNA damage while simultaneously bearing its burden. Cell Death Discov *10*, 436. 10.1038/s41420-024-02206-w.
13. Zheng, L., Dai, H., Zhou, M., Li, X., Liu, C., Guo, Z., Wu, X., Wu, J., Wang, C., Zhong, J., et al. (2012). Polyploid cells rewire DNA damage response networks to overcome replication stress-induced barriers for tumour progression. Nat Commun *3*, 815. 10.1038/ncomms1825.
14. Shu, Z., Row, S., and Deng, W.M. (2018). Endoreplication: The Good, the Bad, and the Ugly. Trends Cell Biol *28*, 465-474. 10.1016/j.tcb.2018.02.006.
15. Herriage, H.C., Huang, Y.T., and Calvi, B.R. (2024). The antagonistic relationship between apoptosis and polyploidy in development and cancer. Semin Cell Dev Biol *156*, 35-43. 10.1016/j.semcdb.2023.05.009.
16. Zeng, J., Hills, S.A., Ozono, E., and Diffley, J.F.X. (2023). Cyclin E-induced replicative stress drives p53-dependent whole-genome duplication. Cell *186*, 528-542 e514. 10.1016/j.cell.2022.12.036.

17. Bates, S., Ryan, K.M., Phillips, A.C., and Vousden, K.H. (1998). Cell cycle arrest and DNA endoreduplication following p21Waf1/Cip1 expression. Oncogene *17*, 1691-1703. 10.1038/sj.onc.1202104.
18. Ullah, Z., Lee, C.Y., and Depamphilis, M.L. (2009). Cip/Kip cyclin-dependent protein kinase inhibitors and the road to polyploidy. Cell Div *4*, 10. 10.1186/1747-1028-4-10.
19. Mueller, P.R., Coleman, T.R., Kumagai, A., and Dunphy, W.G. (1995). Myt1: a membrane-associated inhibitory kinase that phosphorylates Cdc2 on both threonine-14 and tyrosine-15. Science *270*, 86-90. 10.1126/science.270.5233.86.
20. McGowan, C.H., and Russell, P. (1995). Cell cycle regulation of human WEE1. EMBO J *14*, 2166-2175. 10.1002/j.1460-2075.1995.tb07210.x.
21. Vassilev, L.T., Tovar, C., Chen, S., Knezevic, D., Zhao, X., Sun, H., Heimbrook, D.C., and Chen, L. (2006). Selective small-molecule inhibitor reveals critical mitotic functions of human CDK1. Proc Natl Acad Sci U S A *103*, 10660-10665. 10.1073/pnas.0600447103.
22. Cornwell, J.A., Crncec, A., Afifi, M.M., Tang, K., Amin, R., and Cappell, S.D. (2023). Loss of CDK4/6 activity in S/G2 phase leads to cell cycle reversal. Nature *619*, 363-370. 10.1038/s41586-023-06274-3.
23. McKenney, C., Lendner, Y., Guerrero Zuniga, A., Sinha, N., Veresko, B., Aikin, T.J., and Regot, S. (2024). CDK4/6 activity is required during G(2) arrest to prevent stress-induced endoreplication. Science *384*, eadi2421. 10.1126/science.adi2421.
24. Kim, K., Armand, J., Kim, S., and Yang, H.W. (2025). E2F activity determines mitosis versus whole-genome duplication in G2-arrested cells. Nat Commun *16*, 6677. 10.1038/s41467-025-62061-w.
25. Gemble, S., Wardenaar, R., Keuper, K., Srivastava, N., Nano, M., Mace, A.S., Tijhuis, A.E., Bernhard, S.V., Spierings, D.C.J., Simon, A., et al. (2022). Genetic instability from a single S phase after whole-genome duplication. Nature *604*, 146-151. 10.1038/s41586-022-04578-4.
26. Saleh, T. (2024). Therapy-induced senescence is finally escapable, what is next? Cell Cycle *23*, 713-721. 10.1080/15384101.2024.2364579.
27. Anatskaya, O.V., and Vinogradov, A.E. (2010). Somatic polyploidy promotes cell function under stress and energy depletion: evidence from tissue-specific mammal transcriptome. Funct Integr Genomics *10*, 433-446. 10.1007/s10142-010-0180-5.
28. Edgar, B.A., Zielke, N., and Gutierrez, C. (2014). Endocycles: a recurrent evolutionary innovation for post-mitotic cell growth. Nat Rev Mol Cell Biol *15*, 197-210. 10.1038/nrm3756.
29. Lee, H.O., Davidson, J.M., and Duronio, R.J. (2009). Endoreplication: polyploidy with purpose. Genes Dev *23*, 2461-2477. 10.1101/gad.1829209.
30. Zhang, J., Qiao, Q., Xu, H., Zhou, R., and Liu, X. (2022). Human cell polyploidization: The good and the evil. Semin Cancer Biol *81*, 54-63. 10.1016/j.semcancer.2021.04.005.
31. Vittoria, M.A., Shenk, E.M., O'Rourke, K.P., Bolgioni, A.F., Lim, S., Kacprzak, V., Quinton, R.J., and Ganem, N.J. (2018). A genome-wide microRNA screen identifies regulators of tetraploid cell proliferation. Mol Biol Cell *29*, 1682-1692. 10.1091/mbc.E18-02-0141.
32. Sanz-Gomez, N., Gonzalez-Alvarez, M., De Las Rivas, J., and de Carcer, G. (2023). Whole-Genome Doubling as a source of cancer: how, when, where, and why? Front Cell Dev Biol *11*, 1209136. 10.3389/fcell.2023.1209136.
33. Russo, M., Crisafulli, G., Sogari, A., Reilly, N.M., Arena, S., Lamba, S., Bartolini, A., Amodio, V., Magri, A., Novara, L., et al. (2019). Adaptive mutability of colorectal cancers in response to targeted therapies. Science *366*, 1473-1480. 10.1126/science.aav4474.
34. Pienta, K.J., Hammarlund, E.U., Axelrod, R., Amend, S.R., and Brown, J.S. (2020). Convergent Evolution, Evolving Evolvability, and the Origins of Lethal Cancer. Mol Cancer Res *18*, 801-810. 10.1158/1541-7786.MCR-19-1158.
35. McPherson, A., Vazquez-Garcia, I., Myers, M.A., Al-Rawi, D.H., Zatzman, M., Weiner, A.C., Freeman, S., Mohibullah, N., Satas, G., Williams, M.J., et al. (2025). Ongoing genome

doubling shapes evolvability and immunity in ovarian cancer. Nature *644*, 1078-1087. 10.1038/s41586-025-09240-3.
36. Mallin, M.M., Kim, N., Choudhury, M.I., Lee, S.J., An, S.S., Sun, S.X., Konstantopoulos, K., Pienta, K.J., and Amend, S.R. (2023). Cells in the polyaneuploid cancer cell (PACC) state have increased metastatic potential. Clin Exp Metastasis *40*, 321-338. 10.1007/s10585-023-10216-8.
37. Mallin, M.M., Rolle, L.T.A., Schmidt, M.J., Priyadarsini Nair, S., Zurita, A.J., Kuhn, P., Hicks, J., Pienta, K.J., and Amend, S.R. (2025). Cells in the Polyaneuploid Cancer Cell State Are Prometastatic. Mol Cancer Res *23*, 219-235. 10.1158/1541-7786.MCR-24-0689.
38. Fei, F., Zhang, M., Li, B., Zhao, L., Wang, H., Liu, L., Li, Y., Ding, P., Gu, Y., Zhang, X., et al. (2019). Formation of Polyploid Giant Cancer Cells Involves in the Prognostic Value of Neoadjuvant Chemoradiation in Locally Advanced Rectal Cancer. J Oncol *2019*, 2316436. 10.1155/2019/2316436.
39. Coward, J., and Harding, A. (2014). Size Does Matter: Why Polyploid Tumor Cells are Critical Drug Targets in the War on Cancer. Front Oncol *4*, 123. 10.3389/fonc.2014.00123.
40. Zachariae, W., Schwab, M., Nasmyth, K., and Seufert, W. (1998). Control of cyclin ubiquitination by CDK-regulated binding of Hct1 to the anaphase promoting complex. Science *282*, 1721-1724. 10.1126/science.282.5394.1721.
41. Wang, Q., Bode, A.M., and Zhang, T. (2023). Targeting CDK1 in cancer: mechanisms and implications. NPJ Precis Oncol *7*, 58. 10.1038/s41698-023-00407-7.
42. Massacci, G., Perfetto, L., and Sacco, F. (2023). The Cyclin-dependent kinase 1: more than a cell cycle regulator. Br J Cancer *129*, 1707-1716. 10.1038/s41416-023-02468-8.
43. Hirai, H., Arai, T., Okada, M., Nishibata, T., Kobayashi, M., Sakai, N., Imagaki, K., Ohtani, J., Sakai, T., Yoshizumi, T., et al. (2010). MK-1775, a small molecule Wee1 inhibitor, enhances anti-tumor efficacy of various DNA-damaging agents, including 5-fluorouracil. Cancer Biol Ther *9*, 514-522. 10.4161/cbt.9.7.11115.
44. Ghelli Luserna di Rora, A., Cerchione, C., Martinelli, G., and Simonetti, G. (2020). A WEE1 family business: regulation of mitosis, cancer progression, and therapeutic target. J Hematol Oncol *13*, 126. 10.1186/s13045-020-00959-2.
45. Wiederschain, D., Wee, S., Chen, L., Loo, A., Yang, G., Huang, A., Chen, Y., Caponigro, G., Yao, Y.M., Lengauer, C., et al. (2009). Single-vector inducible lentiviral RNAi system for oncology target validation. Cell Cycle *8*, 498-504. 10.4161/cc.8.3.7701.

Figure 1. Genotoxic chemotherapy induces mitotic bypass and endoreplication

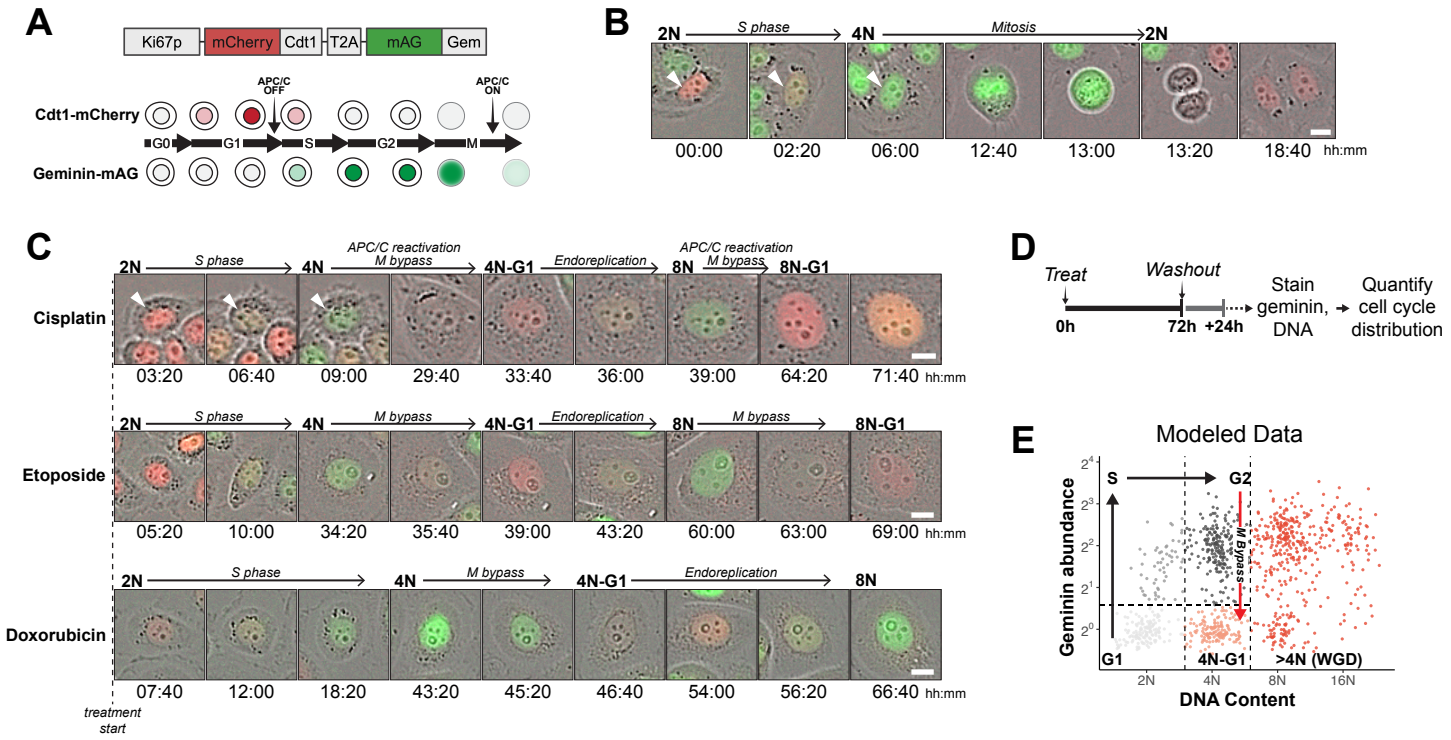

Figure 1. Genotoxic chemotherapy induces mitotic bypass and endoreplication.

A. Schematic of Ki67-T2A-FUCCI reporter and timeline of expression during cell cycle.

B. Example time series shows reporter activity during a normal cell cycle in PC3-FUCCI. Scale bar, 10μm.

C. Example time series shows mitotic bypass and endoreplication in PC3-FUCCI during 72h treatment with cisplatin, etoposide, or doxorubicin. Scale bar, 10μm.

D. Experimental outline for quantifying frequency of mitotic bypass after genotoxic chemotherapy.

E. Model of DNA content vs. geminin abundance scatterplot with gating strategy and interpretation: 2N, geminin(-) cells are in G1; between 2N and 4N, geminin(+) cells are in S; 4N, geminin(+) cells are in G2; 4N, geminin(-) cells have bypassed M into 4N-G1; cells with >4N DNA content have endoreplicated. Colors correspond to plot in (**G**).

F. Scatter plots of DNA content vs. geminin abundance in individual surviving PC3 24h after 72h treatment with the indicated drugs. Points colored based on their relative density. Dotted lines represent cut-off values for DNA content and geminin positivity. Data shown are combined from 3 independent experiments, 1000 individual data points shown for each condition.

G. Quantification of percent of cells in each cell cycle phase in PC3 from (**F**). Data shown are mean percentages from 3 independent experiments.

H. Example time series of PC3-FUCCI undergoing mitotic catastrophe in response to cisplatin treatment. Scale bar, 10μm.

I. Model of chemotherapy-induced premature APC/C reactivation and mitotic bypass compared to normal progression through mitosis. Colors of nuclei represent FUCCI reporter expression.

Figure 2. Cells that persist after genotoxic chemotherapy enter an endocycle

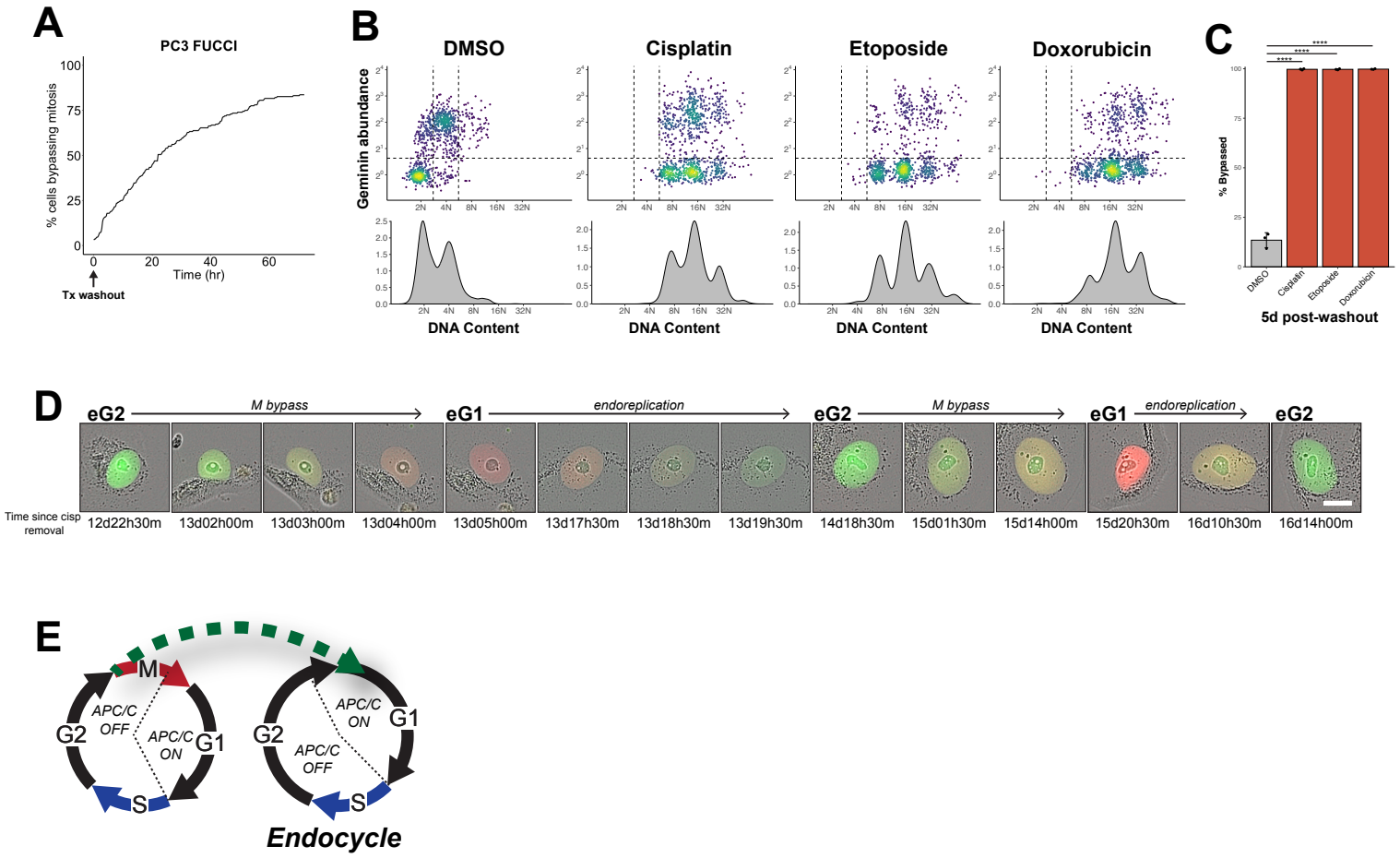

Figure 2. Cells that persist after genotoxic chemotherapy enter an endocycle

A. Cumulative percent of PC3-FUCCI cells that activate APC/C without undergoing mitosis in the 72hr following cisplatin treatment. N= 196 cells.

B. Scatter plots of DNA content vs. geminin abundance in surviving PC3 5 days after cisplatin, etoposide, or doxorubicin treatment with DNA content density distributions underlaid. Points are colored based on their relative density. Data are combined from 3 independent experiments, with 1000 individual nuclei shown per condition.

C. Quantification of the percent of cells that had bypassed mitosis in (**B**). Data are mean +/- sd from 3 independent experiments. Total cells analyzed = 1779 (DMSO); 1191 (cisplatin); 887 (etoposide); 982 (doxorubicin). p values calculated by one-way ANOVA and Dunnett's post-hoc test comparing each treated condition to DMSO control. ****, $p<0.0001$.

D. Representative images of surviving PC3-FUCCI continuing to bypass mitosis and endoreplicate out to >16 days after cisplatin treatment. eG1, endo-G1; eG2, endo-G2. Scale bar, 20μm.

E. Model of surviving cells' transition to chemo-induced endocycle.

Figure 3. WEE1-, Myt1- dependent CDK1 inhibition is required for G2 arrest and mitotic bypass

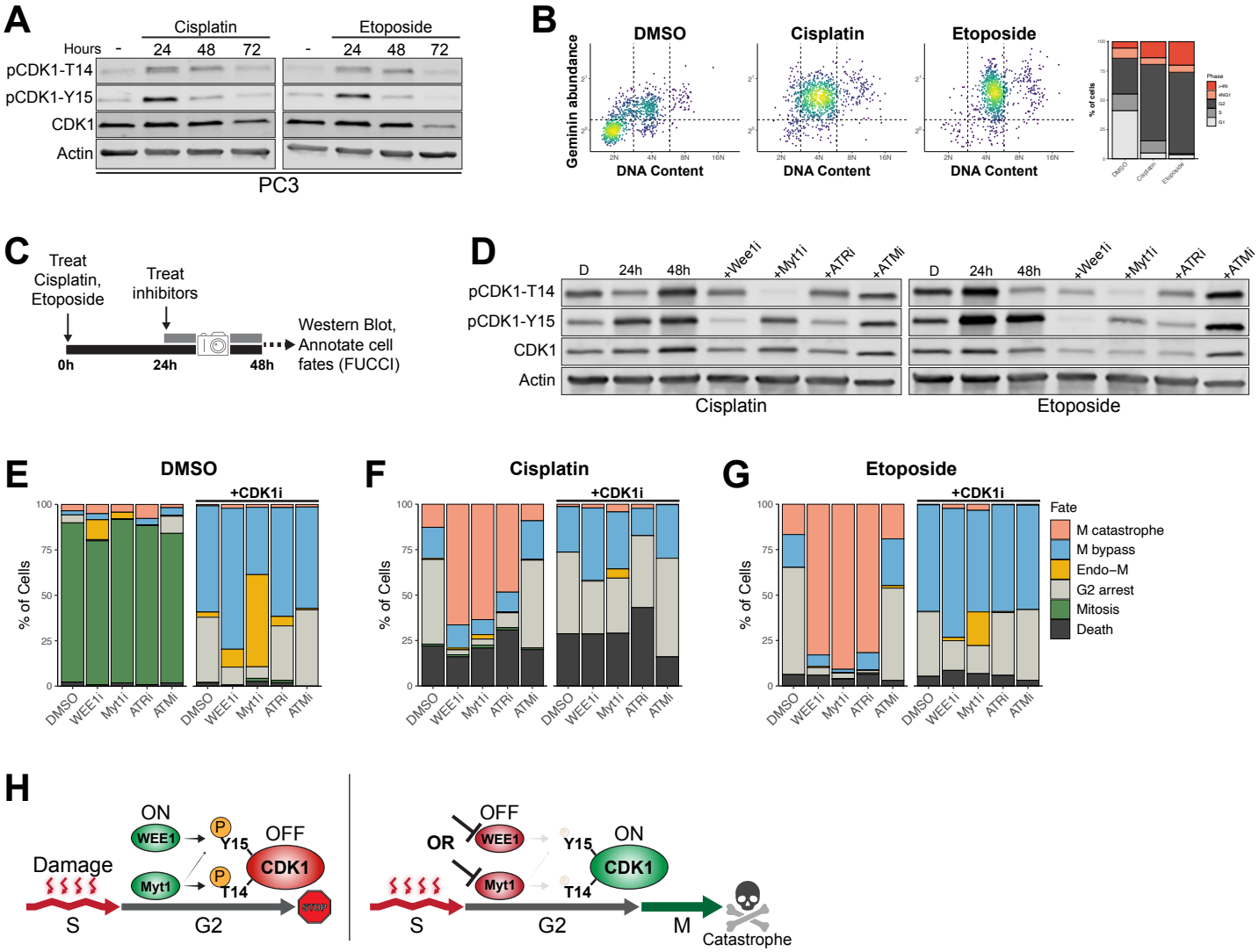

Figure 3. WEE1-, Myt1-dependent CDK1 inhibition is required for G2 arrest and mitotic bypass.

A. Western Blot analysis of CDK1 phosphorylation in PC3 after 24-, 48-, or 72-hour treatment with cisplatin or etoposide. D, DMSO; p, phosphorylation.

B. Left: Scatter plots of DNA content vs. geminin abundance in PC3 treated 24h with the indicated drugs. Points are colored based on their relative density. 1000 individual data points shown for each condition. Right: quantification of percent of cells in each cell cycle phase.

C. Experimental outline for the analysis of the effects of WEE1, Myt1, ATR, or ATM inhibition on cisplatin or etoposide-induced CDK1 phosphorylation and cell fate.

D. Western Blot of PC3 treated as in (**B**) showing the effects of WEE1i, Myt1i, ATRi, and ATMi on cisplatin- or etoposide-induced CDK1 phosphorylation.

E-G. Stacked bar plots showing the fates of PC3-FUCCI after DMSO (**D**), cisplatin (**E**), or etoposide (**F**) +/- inhibitor treatments as depicted in (**C**). Data shown are the mean percent of cells with each fate from $\geq$ 2 independent experiments.

H. Model of DNA damage-induced CDK1 inhibition (left) and the effects of WEE1 or Myt1 inhibition (right).

Figure 4. CDK1 inhibition is sufficient to induce G2 arrest and premature APC/C reactivation

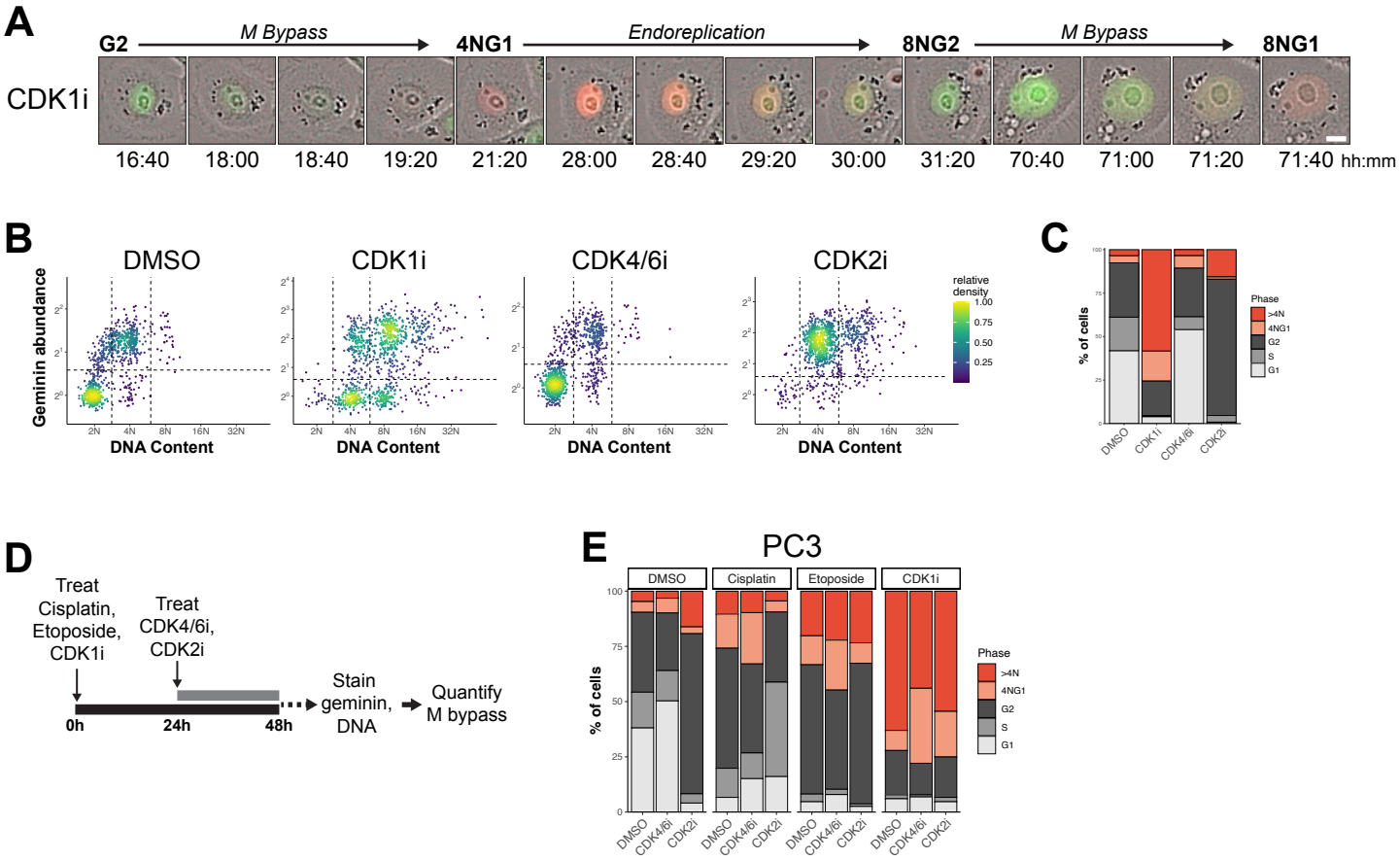

Figure 4. CDK1 inhibition is sufficient to induce G2 arrest and premature APC/C reactivation.

A. Representative time-lapse images of PC3-FUCCI undergoing mitotic bypass and endoreplication during 72h treatment with CDK1i. Scale bar, 10μm.

B. Scatter plots of DNA content vs. geminin abundance in individual PC3 after 72h treatment with DMSO, CDK1i, CDK4/6i, or CDK2i. Points colored based on their relative density. Dotted lines represent cut-off values for determining DNA content and geminin positivity. Data shown are combined from 3 independent experiments. 1000 individual nuclei shown for each condition.

C. Quantification of percent of cells in each cell cycle phase in each condition from (**B**). Data shown are mean percentages from 3 independent experiments.

D. Experimental outline for determining the effects of CDK4/6i or CDK2i on cisplatin-, etoposide-, or CDK1i-induced mitotic bypass.

E. Percent of PC3 in each cell cycle phase after treatment as in (**D**). Data shown are mean percentages from ≥ 5 independent experiments.

Figure 5. Polyploidy and persistent DNA damage induce stress signaling during endo-S phase

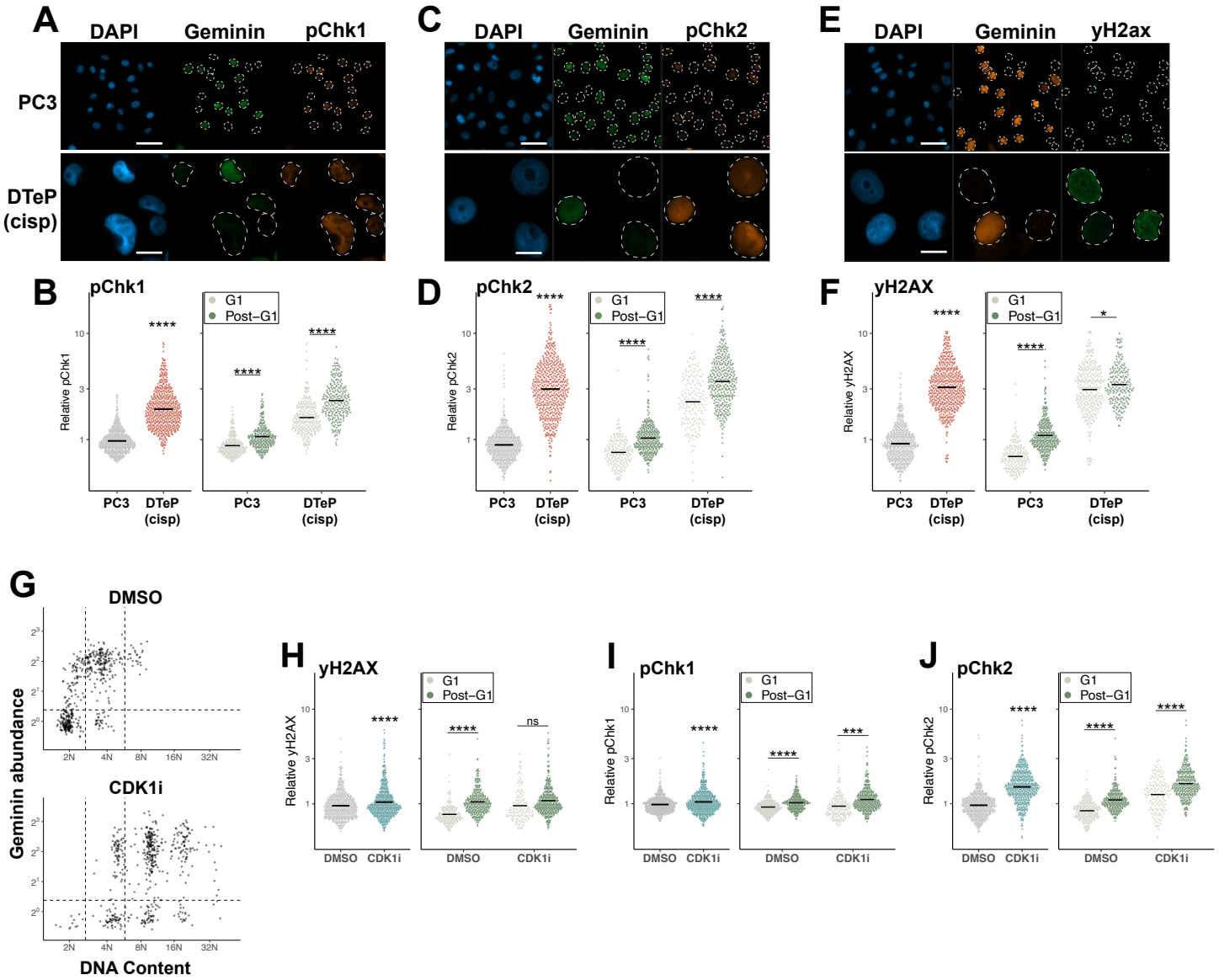

Figure 5. Polyploidy and persistent DNA damage induce stress signaling during endo-S phases.

A. Representative images of PC3 and DTePs 8 days post-cisplatin treatment co-immunostained for geminin and pChk1. Scale bar, 50μm.

B. Quantification of pChk1 abundance in individual nuclei from untreated PC3 and DTePs 8 days post-cisplatin treatment (left) and same data with cells classified as G1 or post-G1 based on geminin abundance (right). Data are combined from 2 independent experiments. Mean for each group indicated by black line. p values calculated by Welch's *t* test (left: DTeP vs. PC3; right: Post-G1 vs. G1 within each group). ****, $p<0.0001$.

C. Representative images of PC3 DTePs 8 days post-cisplatin treatment co-immunostained for geminin and pChk2. Scale bar, 50μm.

D. Quantification of pChk2 abundance as in (**B**).

E. Representative images of PC3 DTePs 8 days post-cisplatin treatment co-immunostained for geminin and yH2AX. Scale bar, 50μm.

F. Quantification of yH2AX abundance as in (**B**). *, $p<0.05$.

G. Scatter plots of DNA content vs. geminin abundance in individual PC3 after 72h DMSO or CDK1i treatment. Data are combined from 2 independent experiments, 500 individual nuclei shown per condition.

H. Quantification of yH2AX abundance in individual nuclei from PC3 treated 72h with DMSO or CDK1i (left) and same data with cells classified as G1 or post-G1 based on geminin abundance (right). Data are combined from 2 independent experiments, 500 individual nuclei shown per drug condition. Mean for each group indicated by black line. p values calculated by Welch's *t* test (left: CDK1i vs. PC3; right: Post-G1 vs. G1 within each drug treatment group). ****, $p<0.0001$; ns, not significant.

I. Quantification of pChk1 abundance in individual nuclei, as in (**H**). ****, $p<0.0001$; ***, $p<0.001$.

J. Quantification of pChk2 abundance in individual nuclei, as in (**H**). ****, $p<0.0001$.

Figure 6. WEE1, Myt1 activities are required for endocycling and survival in persistent cells

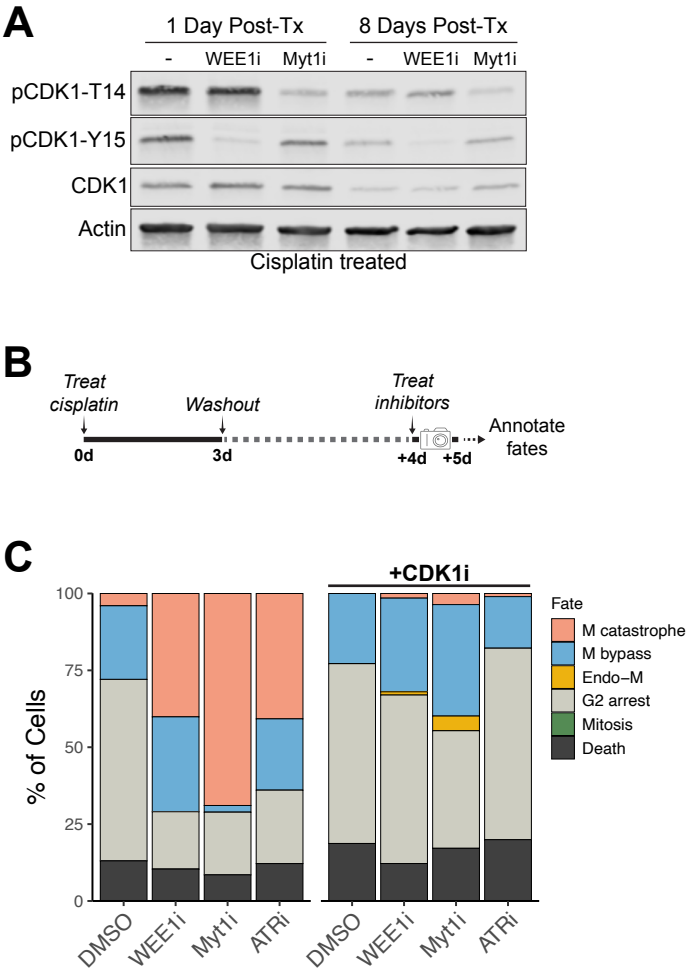

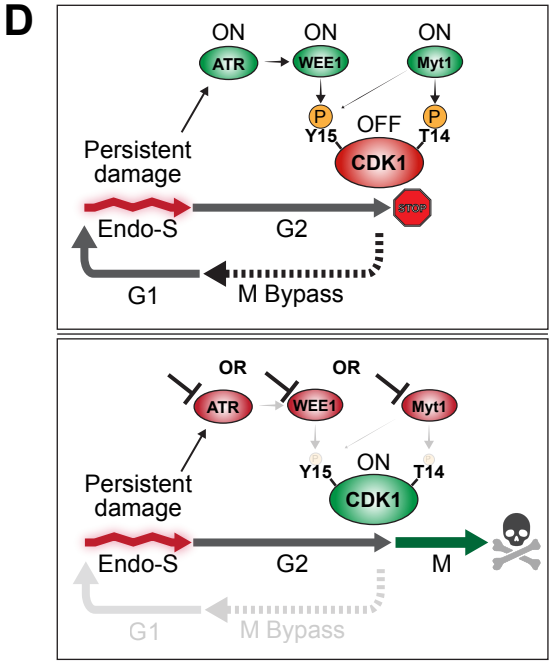

Figure 6. WEE1, Myt1 activities are required for endocycling and survival in persistent cells

A. Western Blot analysis of the effects of WEE1i or Myt1i on CDK1 phosphorylation in ECCs 1- or 8-days post cisplatin treatment.

B. Experimental timeline for analysis of functional effects of WEE1i or Myt1i on ECCs: PC3-FUCCI were treated for 3 days with cisplatin after which drug was washed out. 4 days later, surviving cells were treated with WEE1i, Myt1i, or ATRi +/- CDK1i for 24 hours and timelapse imaged. Cell fates were then manually annotated.

C. Quantification of fates of PC3-FUCCI treated as in (**B**). Data shown are the mean percent of cells with each fate from 3 individual experiments.

D. Model of proposed mechanism of control of the endocycle in DTePs: persistent DNA damage induces stress signaling during endo-S phase, which leads to CDK1 phosphorylation, G2 arrest, and premature APC/C reactivation (mitotic bypass). When treated with WEE1i, Myt1i, or ATRi, ECCs fail to arrest in G2 and instead enter mitosis where they undergo mitotic catastrophe and cell death.